



## Angular Distribution of L Alpha and L Beta X-Rays of Antimony at 59.54 keV

Tuba Akkuş<sup>\*1</sup>, Mesut Alkan<sup>2</sup>, Yusuf Şahin<sup>3</sup>

<sup>1</sup>Department of Physics, Arts and Sciences Faculty, Erzincan Binali Yıldırım University, Erzincan, Turkey.

<sup>2</sup>Department of Physics, Graduate School of Natural and Applied Sciences, Erzincan Binali Yıldırım University, Erzincan, Turkey

<sup>3</sup>Department of Physics, Faculty of Sciences, Ataturk University, Erzurum, Turkey

(Alınış / Received: 13.03.2021, Kabul / Accepted: 20.04.2021, Online Yayınlanma / Published Online: 30.06.2021)

\*Corresponding Author: [takkus@erzincan.edu.tr](mailto:takkus@erzincan.edu.tr), [tuba.akkus@atauni.edu.tr](mailto:tuba.akkus@atauni.edu.tr) (T. Akkuş)

(ORCID: <https://orcid.org/0000-0003-3913-5562>)

### Keywords

Antimony,  
Scattering Angle,  
L X-rays,  
Anisotropy,  
Alignment

**Abstract:** The L alpha and L beta differential cross-section of antimony have been calculated at an angular range 85° -135° at 59.54 keV. It was observed that L alpha differential cross sections of had an anisotropic distribution namely it was depend on the angles but L beta differential cross sections had an isotropic distribution. The anisotropy and alignment parameter of antimony were obtained from intensity ratio.

## Antimonun 59.54 keV'de L Alfa ve L Beta X-Işınlarının Açısız Dağılımı

### Anahtar

### Kelimeler

Antimon,  
Saçılma Açısı,  
L X-ışınları,  
Anizotropi,  
Hizalama

**Özet:** Antimonun L alfa ve L beta diferansiyel tesir kesitleri 59,54 keV'de 85°-135° açısız aralıkta hesaplanmıştır. L alfa diferansiyel kesitlerinin anizotropik bir dağılıma sahip olduğu, yani açığa bağlı olduğu, ancak L beta diferansiyel kesitlerinin izotropik bir dağılıma sahip olduğu görülmüştür. Antimonun anizotropi ve hizalanma parametreleri şiddet oranından elde edildi.

### 1. Introduction

Antimony is a semi-metallic element in the 5A group on the periodic table. It can found in two different forms. These are metallic and non-metallic forms. Antimony is rarely found in nature, it is often found in association with arsenic and bismuth because of its similarity. The areas of application of antimony are quite extensive. It is widely used in semiconductors, thermoelectric devices, accumulators, soldering, printing machine letters, military supplies, matches, rubber, fabric dyes, steel products, pigments, bullets, textile products, markers, bullets, electric wire coatings, diodes, infrared detectors, brakes boats, pillows, fishing tackle and toys. Although antimony has wide application areas, various health problems can be seen in people working with antimony. The exposure to antimony can cause serious health problems such as heart problems, lung diseases.

Experimental and theoretical studies of the angular dependence were investigated by researchers for many years. First, in 1969, Cooper and Zare proposed a theoretical model for the alignment of atoms excited by photons. In this theoretical model, they predict the vacancy states with  $j=1/2$  are unaligned and accordingly the emission of x-rays are isotropic and unpolarized [1]. After three years, in 1972, Flügge and colleagues proposed different theoretical view. This view predicts that the decay states with angular momentum  $j>1/2$  are aligned and x-rays emission following the vacancy state are anisotropic and polarized [2]. Thus, the K shell and  $L_1$  and  $L_2$  sub shell vacancy states with  $j=1/2$  will be unaligned but the  $L_3$  sub-shell vacancy states with  $j>1/2$  will be aligned. Some researchers have done theoretical investigation on this subject [3-6]. The theoretical studies of these researchers have been experimentally supported by some researchers [7-11]. Experimental studies usually

involve measurements of the polarization or angular distribution of the excited x-rays [12-17].

In recent years, Requena and Williams [18] investigated the angular distribution of photon-induced Au in the angular range 25°-155°. The angular dependence of L x-rays bombarded 18-60 MeV fluorine ions was investigated for Au, Pb and Bi [19]. Sharma and Mittal [20] investigated alignment of tungsten near  $L_3$  sub-shell threshold using theoretical, experimental and empirical methods for azimuthal angle of 0°, 30°, 60°, 90° and 120°. Sestric et al. [21] have studied angular distribution of Au in angular range 0°-25°. They found that the angular distribution of the  $L_\alpha$  and  $L_\beta$  x-rays are essentially isotropic and  $L_\gamma$  x-rays may be weakly anisotropic.  $L_3$  sub-shell alignment induced by swift silicon ions was investigated for Bi by Kumar et al. [22]. In this work, they found that  $L_\alpha$  and  $L_\beta$  x-rays are isotropic and  $L_\gamma$  x-rays are anisotropic. Wang et al. [23] investigated angular dependence of L x-rays of Ag. They found that  $L_{\beta_1}$ ,  $L_{\beta_2}$  and  $L_{\gamma_1}$  x-rays are isotropic while the  $L_\alpha$  x-rays are anisotropic.

It can be seen from the literature review that theoretical and experimental studies about the angular distribution and alignment of x-rays are incompatible also the calculated values of the atomic parameters (cross section, polarization, alignment etc.) are different from each other. In the literature, there is not study about the angular dependence of antimony.

## 2. Materials and Method

The experimental set up used in the present study is shown in Figure 1. The polar scattering angles are

measured in the range  $85^\circ \leq \theta \leq 135^\circ$  with  $10^\circ$  steps. At all measurements the source and target were together rotated around the z axis. The detector was kept in the same position during measurements. The detector is shielded by a lead collimator to avoid direct exposure of it from the radiation incoming from the source and environment. An  $\text{Am}^{241}$  radioactive point source with activity 100 mCi was used to irradiated the samples. The measuring time for each angle was 86400 s. The emitted x-rays and scattered photons were detected by a high purity germanium detector has a resolution of 199.6 eV at the 5.9 keV, with active area 200 mm<sup>2</sup> and beryllium window of 12.5  $\mu\text{m}$  thickness.

We are used to the computer program Genie-2000 to acquire the spectra and to control the operating parameters of the system. Microcal Origin 8.5 Software program was used to determine the peak areas. This program uses least square fit method in order to determine the net peak areas. The background spectrum was measured for each angle and subtracted from the raw spectrum to correct the background in the peak region. The typical spectra acquired of antimony is shown in Figure 2.

The  $I_0 G \epsilon$  values were determined by measuring the K x-rays obtained from spectroscopically pure targets for all polar scattering angle. The experimental differential cross-sections for L x-rays were calculated using the following equation

$$\frac{d\sigma(L_i)}{d\Omega} = \frac{N_{L_i}}{4\pi I_0 G \epsilon \beta_{L_i}} \quad (1)$$

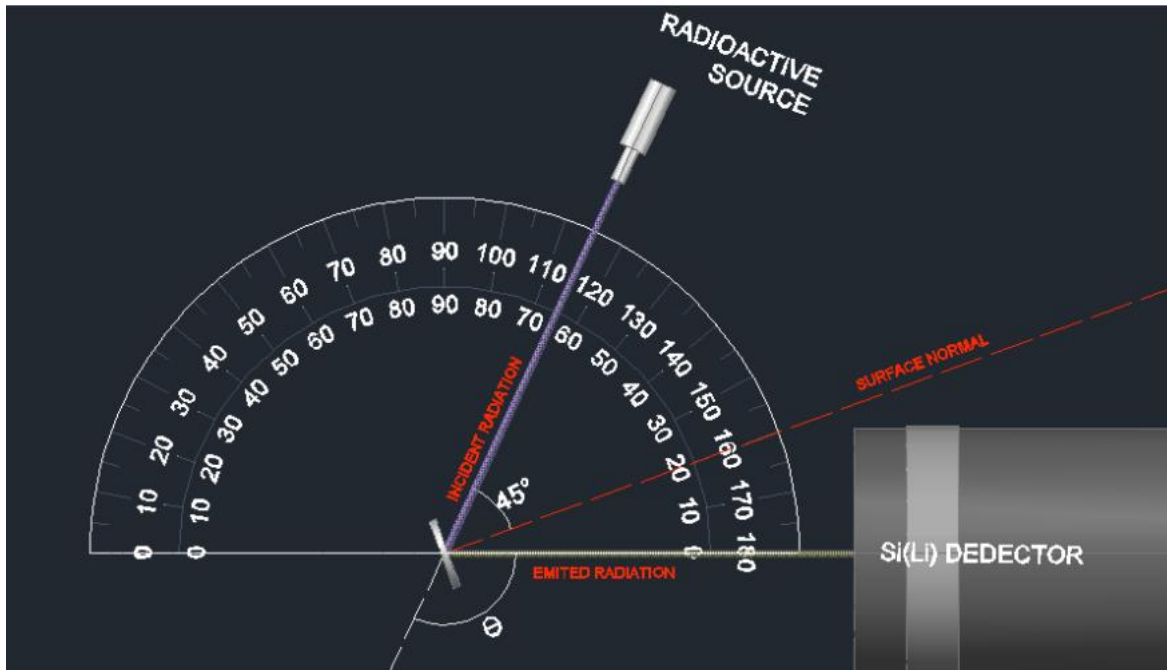
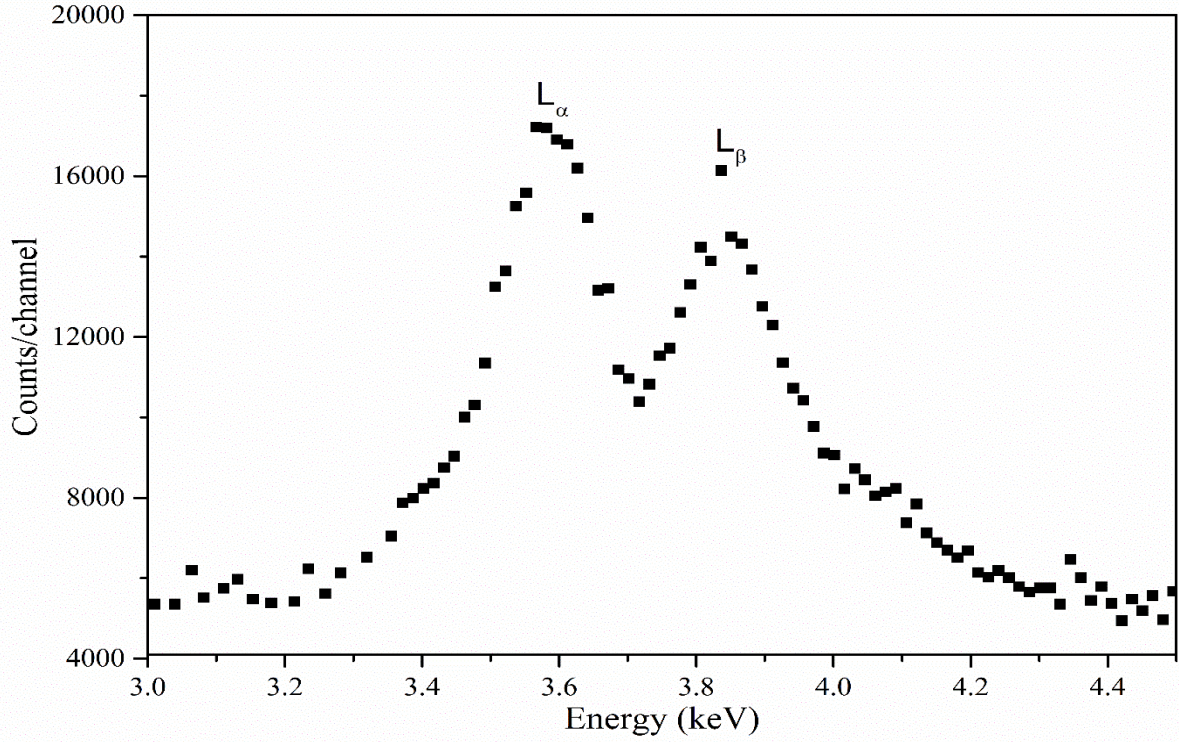


Figure 1. The experimental set up for  $\theta=115^\circ$ .



**Figure 2.** The typical spectrum of antimony.

where  $N_{L_i}$  is the number of L x-rays detected per second in the  $L_i$  x-ray peak,  $I_0G$  is the intensity of photons incoming on the portion of the target visible to the detector.  $\varepsilon$  is the detector efficiency at  $L_i$  x-ray energy,  $t$  is the thickness of the target.  $\beta_{L_i}$  is the target self-absorption correction factor and calculate using the following equation,

$$\beta = \frac{1 - \exp\left[(-1)\left(\frac{\mu_i}{\cos\theta_1} + \frac{\mu_e}{\cos\theta_2}\right)t\right]}{\left(\frac{\mu_i}{\cos\theta_1} + \frac{\mu_e}{\cos\theta_2}\right)t} \quad (2)$$

where  $\mu_i$  and  $\mu_e$  are the total mass absorption coefficients of incident photons and emitted characteristic x-rays. The values of  $\mu_i$  and  $\mu_e$  are taken from WinXCom [24].  $\theta_1$  and  $\theta_2$  are the angles of incident gamma-ray and emitted K x-rays with the sample normal, respectively. Also,  $t$  is the mass thickness of the sample.

The effective incident photon flux factor,  $I_0G\varepsilon$  was determined by using the following equation

$$I_0G\varepsilon_{K_i} = \frac{N_{K_i}}{\beta_{K_i}\sigma_{K_i}t} \quad (3)$$

where  $N_{K_i}$  is the net number of counts under the  $K_\beta$  or  $K_\alpha$  peaks,  $\sigma_{K_i}$  is the  $\sigma_{K_\alpha}$  or  $\sigma_{K_\beta}$  fluorescence cross

section.  $I_0$  is the intensity of incident radiation,  $G$  is the geometrical factor,  $\varepsilon_{K_i}$  is the detector efficiency for  $K_i$  x-rays. The theoretical values of  $\sigma_{K_\alpha}$  or  $\sigma_{K_\beta}$  fluorescence cross sections were calculated by using the following equations

$$\sigma_{K_\alpha} = \sigma_{K_E}w_Kf_{K_\alpha} \quad (4)$$

$$\sigma_{K_\beta} = \sigma_{K_E}w_Kf_{K_\beta} \quad (5)$$

where  $\sigma_{K_E}$  is the K shell photoionization cross section for the given elements at the excitation energy  $E$ . In this work, the values of  $\sigma_{K_E}$  were taken from Scofield [25] and the values of  $w_K$  were taken from the report by Hubbell et al. [26]. The fractional emission ratio of the  $K_\alpha$  and  $K_\beta$  x-rays,  $f_{K_\alpha}$  and  $f_{K_\beta}$  are taken from Scofield [27]

$$f_{K_\alpha} = \left(1 + I_{K_\beta}/I_{K_\alpha}\right)^{-1} \quad (6)$$

$$f_{K_\beta} = \left(1 + I_{K_\alpha}/I_{K_\beta}\right)^{-1} \quad (7)$$

The fitted curves for all polar scattering angles are shown in Figure 3.

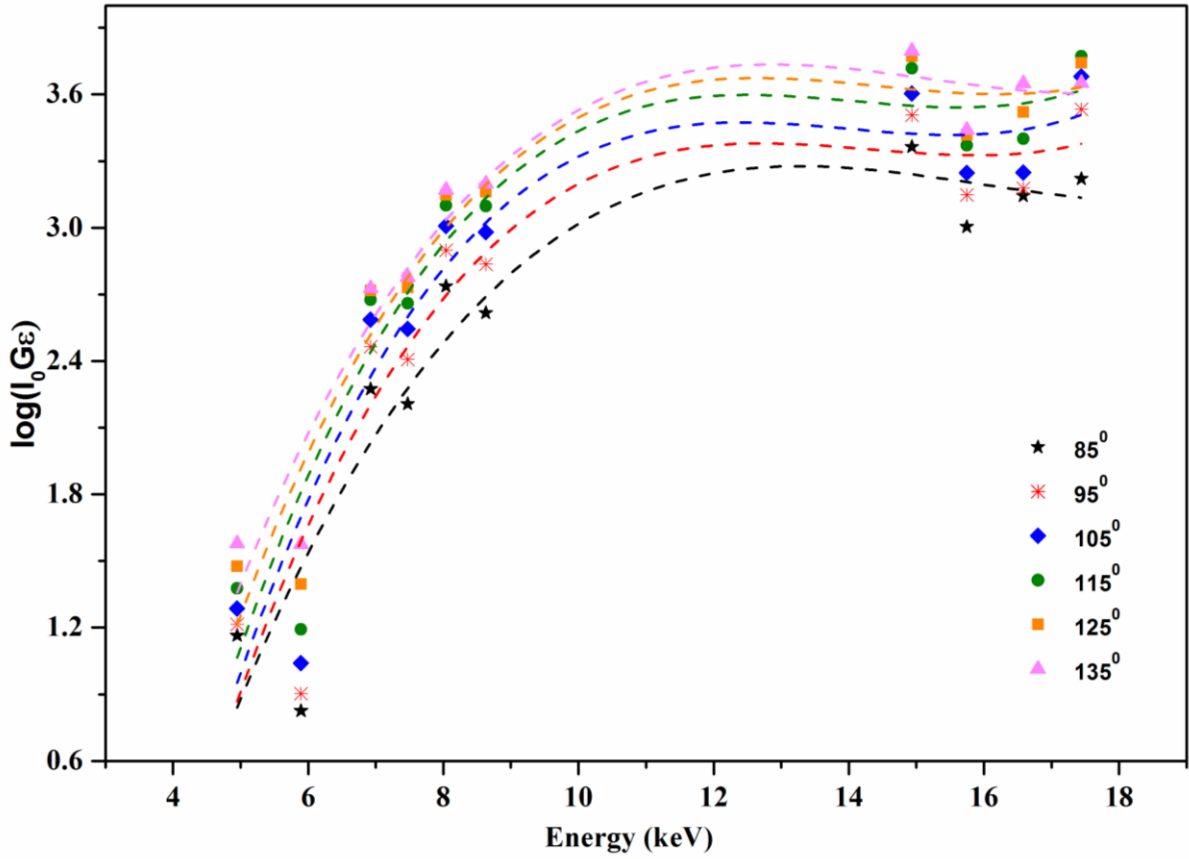


**Figure 3.** The variation of the factor  $I_0 G\epsilon$  as a function of energy for all scattering angles.

The anisotropy and alignment parameters for antimony with the following equation

$$I(\theta) = \frac{I_0}{4\pi} [1 + \beta_A P_2(\cos\theta)] \quad (8)$$

$P_2(\cos\theta)$  and  $\beta_A$  are the Legendre polynomial and anisotropy parameter, respectively.

$$\beta_A = \alpha \kappa A_2 \quad (9)$$

where  $A_2$ ,  $\kappa$  and  $\alpha$  are the alignment parameter, Coster-Kronig correction factor and a coefficient depends only on the total angular momenta of the initial and final state of the photoionized atom, respectively.

The differential x-ray intensity is predicted to have a linear dependence with the  $P_2(\cos\theta)$  term in the case of anisotropic emission and would retain same linear behavior if the x-rays intensity is normalized to the intensity of any isotropically emitted x-rays [22]. From the differential cross section of this study, we found that the emission of  $L_\beta$  x-rays are isotropic. The intensity ratios  $I_{L_\alpha}/I_{L_\beta}$  is plotted as a function of  $P_2(\cos\theta)$  for antimony which have seen in Figure 5.

As seen from equation 8 the linear least square fit of x-ray intensity ratios as a function of  $P_2(\cos\theta)$  provides  $\beta_A$  value. The  $A_2$  alignment parameter is found by

equation 9. In this equation  $\alpha$  is a coefficient.  $\kappa$  is the Coster-Kronig correction factor ;

$$\kappa = 1 + f_{23} \frac{\sigma_{L_2}}{\sigma_{L_3}} + (f_{13} + f_{12}f_{23}) \frac{\sigma_{L_1}}{\sigma_{L_3}} \quad (10)$$

where  $\sigma_{L_i}$  ( $i = 1,2,3$ ) is the ionization cross-section in the  $L_i$  subshell and  $f_{ij}$  is the Coster-Kronig transition probability. The values of  $\sigma_{L_i}$  and  $f_{ij}$  were taken from Scofield [25] and Krause [28] respectively.

### 3. Results and Discussion

In this study, we calculated L alpha ( $L_\alpha$ ) and L beta ( $L_\beta$ ) differential cross section of antimony at different scattering angles (85°, 95°, 105°, 115°, 125° and 135°). As can be seen from Figure 4, angular dependence of L alpha and L beta x rays. We have confirmed that the L alpha x rays are depend on the angles and the L beta x rays are not depend on the angles. These results are expected because the vacancy state having a total angular momentum greater than 1/2 formed by direct photoionization may be aligned and the x-rays to be emitted from such an aligned vacancy may also exhibit anisotropic angular distribution. The vacancy states with  $J = 1/2$  exhibit an isotropic spatial distribution due to the co-population of magnetic subshells so that emitted x-rays are isotropic.

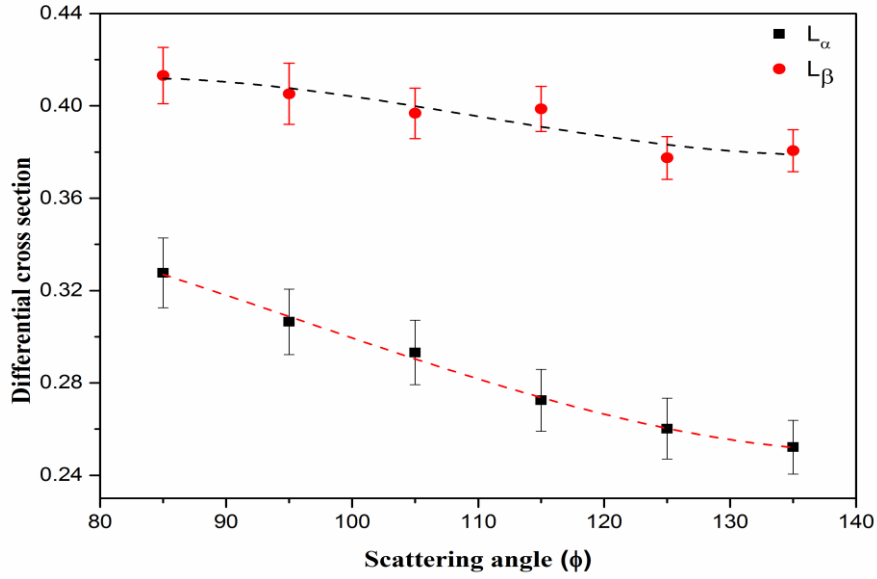


**Figure 4.** The L alpha and L beta differential cross sections of antimony.

Also in this study, the anisotropy parameters provided by the linear least square fit of the x-ray intensity ratios as a function of  $P_2(\text{Cos}\theta)$ . It is clear that the slope of Figure 5 gives the anisotropy parameter ( $\beta_A$ ). The calculated anisotropy and alignment parameter of antimony are given in Table 1. It is quite difficult to

excite the L x rays of the antimony with 59.54 keV photons, because the energy of the antimony L x rays is much smaller than the energy of 59.54 keV photons. Therefore, in the literature, there are no studies in which L x-rays of antimony are excited with 59.54 keV photons.

**Table 1.** Some angular parameters of antimony.

$f_{12}$	$f_{13}$	$f_{23}$	$\sigma_{L_1}$	$\sigma_{L_2}$	$\sigma_{L_3}$	$\kappa$	$\beta_A$	$A_2$
0.17	0.28	0.156	108.316	33.085	33.085	2.116	-0.0986	-0.9319

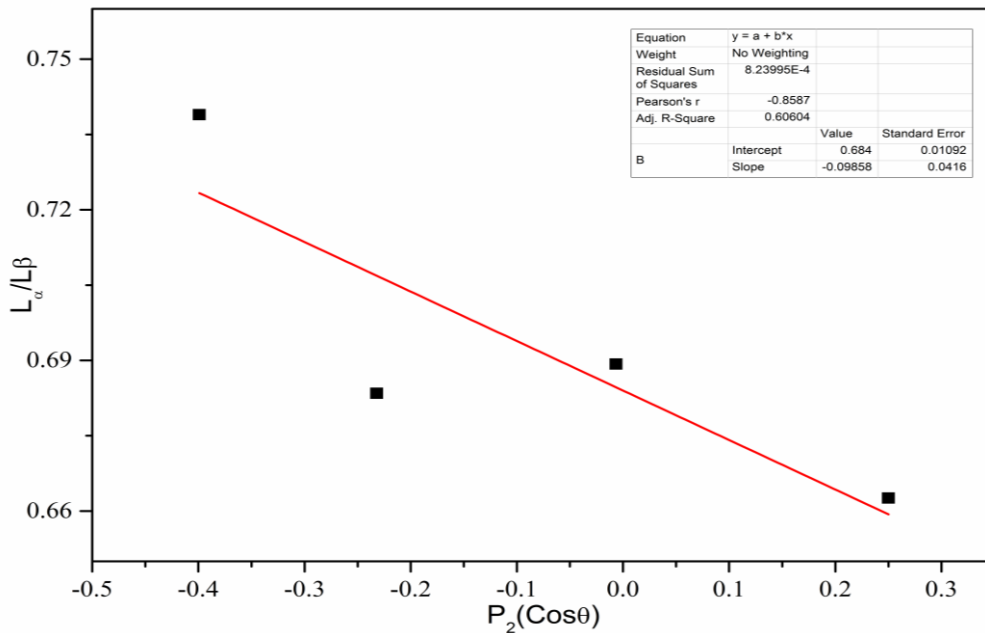


**Figure 5.**  $I_{L_\alpha}/I_{L_\beta}$  intensity ratio versus  $P_2(\text{Cos}\theta)$  for antimony.

#### 4. Conclusion

In the present study, we calculated  $L_\alpha$  and  $L_\beta$  differential cross sections of antimony. As seen from the Figure 4, angular variation of  $L_\beta$  differential cross-sections versus scattering angles is weaker than that of  $L_\alpha$  differential cross-sections. Therefore we can say that the  $L_\alpha$  differential cross-sections show anisotropy but  $L_\beta$  differential cross-sections have isotropy. To the best of our knowledge the anisotropy parameters provided  $L_\alpha/L_\beta$  intensity ratio. The slope of the curve in Figure 5 gives the anisotropy parameter ( $\beta_A$ ).

#### ACKNOWLEDGE

This experimental study was supported by the Scientific Research Project Unit of Ataturk University. (Project number:2016/173)

#### CONFLICT OF INTEREST

The authors declare that they have no known competing financial interests or personal relationships that could have appeared to influence the work reported in this paper.

#### References

- [1] Cooper J, Zare N. Photoelectron angular distributions. In:Geltman, S., Mahanthappa, K.T., Brittin, W.E. (Eds.), Lectures in Theoretical Physics: Atomic Collision Processes, vol. X1C. Gordon and Breach, 1969.
- [2] Flügge S, Mehlhorn W, Schmidt V. Phys. Rev. Lett. 1972; 29 (1):7-9.
- [3] Mehlhorn W. Nucl. Instrum. Methods Phys. Res. B. 1994;87(1-4): 227-31.
- [4] Mc Farlane SC. J. Phys. B At. Mol. Opt. Phys. 1972; 5:1906-15.
- [5] Berezhko EG, Kabachnik NM. J. Phys. B: At. Mol. Opt. Phys. 1977;10:2467-77.
- [6] Sizov V, Kabachnik NM. J. Phys. B: At. Mol. Opt. Phys. 1980; 13:1601.
- [7] Schöler A, Bell F. Z. Phys. A 1978; 286:163-68.
- [8] Pálinkás J, Schlenk B, Valek A. J. Phys. B: At. Mol. Opt. Phys. 1981; 14: 1157-59.
- [9] Wigger J, Altevogt H, Brüssermann M, Richter G, Cleff, B. J. Phys. B: At. Mol. Opt. Phys. 1984; 17:4721. [10] Jesus AP, Ribeiro JP, Niza IB, Lopes JS. J. Phys. B: At. Mol. Opt. Phys. 1989; 22:65.
- [10] Jesus AP, Ribeiro JP, Niza IB, Lopes JS. Phys. B: At. Mol. Opt. Phys. 1989; 22:65.
- [11] Mitra D, Sarkar M, Bhattacharya D, Chatterjee MB, Sen P, Kuri G., Mahapatra, et al. Phys. Rev. A. 1996; 53:2309-13.
- [12] Hardy J, Henins A, Bearden JA. Phys. Rev. A. 1970; 2:1708-10.
- [13] Döbelin E, Sandner W, Mehlhorn W. Phys. Lett. A. 1974; 49:7-8.
- [14] Stachura Z, Bosch F, Hamsch FJ, Liu B, Maor D, Mokler PH, et al. J. Phys. B: At. Mol. Opt. Phys. 1984; 17: 835-47.
- [15] Bhalla CP. Phys. Rev. Lett. 1990; 64:1103-106.
- [16] Mehlhorn W. Nucl. Instrum. Methods Phys. Res. B. 1994; 8: 7227-233.
- [17] Papp T. Nucl. Instrum. Methods Phys. Res. B. 1999;154:300-306.
- [18] Requena S, Williams S. Radiation Physics and Chemistry. 2011;80:629-31.
- [19] Kumar A, Agnihotri AN, Misr D, Kasthurirangan S, Sarkadi L, Tribedi LC. J. Phys. B: At. Mol. Opt. Phys. 2012; 45: 215205.
- [20] Sharma A, Mittal R. Journal of Nuclear Physics, Material Sciences, Radation and Application. 2013; 1:83-101.
- [21] Sestric G, Ferguson S, Wright I, Williams S. Radiat. Phys. Chem. 2014; 102: 40-43.
- [22] Kumar A, Agnihotri AN, Misra D., Kasthurirangan Sarkadi SL, Tribedi LC. J. Phys. B: At. Mol. Opt. Phys. 2015; 48: 065202.
- [23] Wang X., Xu Z, Zhang Y, Ma C, Zhu C. Radiat. Phys. Chem. 2016;125: 102-105.
- [24] Gerward L, Guilbert N, Jensen KB, Levring H. Radiat. Phys. Chem. 2004;71: 653-54.
- [25] Scofield JH. Report No. URCL 51326. Lawrence Livermore Laboratory, Livermore, CA. 1973;1-375.
- [26] Hubbell JH, Trehan PN, Singh N, Chand B, Mehta D, Garg ML, et al. Journal Physics and Chemistry Ref. Data. 1994; 23: 339-64.
- [27] Scofield J.H. Atomic Data Nuclear Data Tables. 1974; 14(2): 121-37.
- [28] Krause MO. J. Phys. Chem. Ref. Data. 1979; 8: 307-27.